Berry Flux Diagonalization: Application to Electric Polarization

John Bonini, David Vanderbilt, and Karin M. Rabe[1]

[1]*Department of Physics and Astronomy, Rutgers University, Piscataway, NJ 08854-8019*

(Dated: February 11, 2020)

The switching polarization of a ferroelectric is a characterization of the current that flows due to changes in polarization when the system is switched between two states. Computation of this change in polarization in crystal systems has been enabled by the modern theory of polarization, where it is expressed in terms of a change in Berry phase as the material switches. It is straightforward to compute this change of phase, but only modulo 2π, requiring a branch choice from among a lattice of values separated by 2π. The measured switching polarization depends on the actual path along which the material switches, which in general involves nucleation and growth of domains and is therefore quite complex. In this work, we present a physically motivated approach for predicting the experimentally measured switching polarization that involves separating the change in phase between two states into as many gauge-invariant smaller phase changes as possible. As long as the magnitudes of these smaller phase changes remain smaller than π, their sum forms a phase change which corresponds to the change one would find along any path involving minimal evolution of the atomic and electronic structure. We show that for typical ferroelectrics, including those that would have otherwise required a densely sampled path, this technique allows the switching polarization to be computed without any need for intermediate sampling between oppositely polarized states.

I. INTRODUCTION

Bistable systems with a change in electric polarization on switching between the two states are of central importance in functional material and device design. The most familiar of such systems are ferroelectrics, with two or more symmetry-related polar insulating states.[1] Switching in systems in which the two states are not symmetry related, for example in antiferroelectrics or heterostructures, is also of great interest for novel devices.[2,3]

First principles prediction of the switching polarization in periodic systems is based on the modern theory of polarization, which expresses the polarization change between two states in terms of the change in Berry phase as the system evolves along a specified adiabatic path.[4,5] Given only the initial and final states, the polarization change is determined modulo the "quantum of polarization" ($e\mathbf{R}/\Omega$), where e is the charge of an electron, $\mathbf{R}$ is a lattice vector, and Ω is the volume of the unit cell. The choice from this set that gives the specific value of the polarization change depends on the actual switching path.

Since the path for a process such as electric field switching of a ferroelectric generally involves nucleation and growth of domains, beyond the scope of current first-principles computation, it might at first seem that first-principles prediction of the switching polarization should not be possible. However, it is an empirical fact that good agreement with experimental observation has been obtained for many ferroelectrics by computing the polarization change along a fictitious minimal path, usually constructed by simple linear interpolation of the atomic positions of the up- and down-polarized states, maintaining their lattice translational symmetries.[6] The polarization change along this fictitious path is then computed by sampling densely enough along the path so that the polarization change for every step along the path can be chosen (and is chosen) to be small compared to the quantum of polarization. However, this method can be computationally intensive, depending on the sampling density required. Moreover, for some systems, it might be that not all the states on the simple linear interpolation path are insulating, and additional effort is required to find an insulating adiabatic path connecting the up and down states. As a result, this approach has proven to be problematic for automated high-throughput applications.

In this paper, we present a new method for predicting switching polarization given only the initial and final states. Our approach uses information, computed from the two sets of ground state wavefunctions, that goes beyond that used in a conventional Berry phase calculation. The key idea is to incorporate certain assumptions about the physical path, eliminating the need to construct a fictitious path and perform calculations for intermediate states. We begin by discussing the method for the simplest case of the electronic contribution to the switching polarization for a one-dimensional polar insulator. We then generalize to three-dimensional materials and discuss the ionic contribution to the polarization. Finally, first-principles results are presented for a realistic benchmark system to illustrate the various aspects of the method and to compare with the fictitious path method. The approach presented here is not limited to computation of switching polarization in ferroelectrics, but can be applied to the change in polarization between two symmetry-inequivalent states, for example in antiferroelectrics, heterostructures and pyroelectrics, and in the computation of the nonlinear response of insulators to electric fields.

II. FORMALISM

A. Background and notation

We start by considering a one-dimensional crystal switching between initial state A and final state B along a specified path parameterized by λ, along which the system remains insulating. According to the modern theory of polarization,[4–7] the electronic contribution to the change in polarization can be expressed as

$$\Delta P_{A\to B} = \frac{-e}{2\pi}\,\Phi \tag{1}$$

where Φ is the Berry flux

$$\Phi = \int\int_S \Omega(k,\lambda)\,d\lambda\,dk \tag{2}$$

obtained by integrating the Berry curvature $\Omega(k,\lambda)$ over the region S with $\lambda_A \le \lambda \le \lambda_B$ and $-\pi/a < k \le \pi/a$ (the first Brillouin zone). Here the Berry curvature

$$\Omega(k,\lambda) = \sum_n -2\mathrm{Im}\,\langle \partial_\lambda u_n(k,\lambda)|\partial_k u_n(k,\lambda)\rangle \tag{3}$$

is written in terms of the cell-periodic parts of the occupied Bloch wavefunctions $|u_n(k,\lambda)\rangle$ and has been traced over the occupied bands n. The $|u_n(k,\lambda)\rangle$ are chosen to be differentiable over the surface S and periodic in k. Application of Stoke's theorem gives

$$\Phi = \oint_C \mathbf{A}(\mathbf{q})\cdot d\mathbf{q} \tag{4}$$

where C is the boundary of the surface S, $\mathbf{q} = (k,\lambda)$, and $\mathbf{A}(\mathbf{q}) = (A_k, A_\lambda)$ is the Berry potential given by

$$A_k = \sum_n i\,\langle u_n(k,\lambda)|\partial_k u_n(k,\lambda)\rangle\ , \tag{5}$$

$$A_\lambda = \sum_n i\,\langle u_n(k,\lambda)|\partial_\lambda u_n(k,\lambda)\rangle\ . \tag{6}$$

Since we have chosen a periodic gauge in the k direction, the two portions of the path C running in the λ direction cancel. The two remaining segments take the form

$$\phi_\lambda = \int_{-\pi/a}^{\pi/a} A_k(k,\lambda)dk \tag{7}$$

and it follows that

$$\Phi = \phi_{\lambda_B} - \phi_{\lambda_A}\ . \tag{8}$$

The electronic contribution to the change in polarization is then given by Eq. (1).

The equivalence of Eq. (8) to Eq. (2) is critically dependent on the gauge choice for the ($|u_n(k,\lambda)\rangle$. A (k,λ)-dependent unitary rotation among the occupied states $|u_n(k,\lambda)\rangle$ can change ϕ_{λ_A} and ϕ_{λ_B}, and their difference, by multiples of 2π,[4–6] so that the change in polarization is determined only modulo the quantum of polarization $e\mathbf{R}/\Omega$. As we describe more fully below, previous methods for making the correct branch choice for a given path rely on implicit construction of a smooth gauge by dense sampling in λ as well as k. Here, we present an alternative approach that makes full use of the information contained in the initial and final states, while eliminating the need for sampling at intermediate values of λ. Moreover, this approach requires a k-space sampling no denser than that required for the computation of the formal polarization.

B. Gauge class

We first consider the case of a single occupied band in 1D with Bloch states $|u(k)\rangle$. Following Eq. (8), the Berry phase around the Brillouin zone at a given λ is given by

$$\phi = \int_{-\pi/a}^{\pi/a} \langle u(k)|i\partial_k u(k)\rangle\,dk \tag{9}$$

The requirement that the gauge be smooth and periodic in k allows transformations of the form $e^{-i\beta(k)}\,|u(k)\rangle$, where $\beta(k)$ is differentiable and $\beta(k+2\pi/a) = \beta(k)+2\pi n$ for some integer n, which changes ϕ by $2\pi n$. For a given physical system, we can test whether two choices of gauge a and b will produce the same value of ϕ by computing

$$\gamma^{\mathrm{ab}}(k) = \langle u^a(k)|u^b(k)\rangle\ . \tag{10}$$

Note that $\gamma^{\mathrm{ab}}(k)$ has exactly unit norm and is just $e^{-i\beta(k)}$, where $\beta(k)$ describes the gauge change relating a to b. If $\gamma^{ab}(k)$ is smooth and its phase does not wind by a nonzero integer multiple of 2π as k traverses the 1D Brillouin zone, the two gauges will produce the same ϕ, and can be said to belong to the same "gauge class."

Next, we consider two crystals A and B with single occupied bands, each with a smooth gauge, and ask whether their respective gauges belong to the same gauge class in a similar sense. With this motivation, we define, in analogy with Eq. (10),

$$\gamma^{AB}(k) = \langle u^A(k)|u^B(k)\rangle \tag{11}$$

where $\gamma^{AB}(k)$ will generally not have unit norm. In fact, for this procedure to be meaningful, systems A and B must be sufficiently closely related that the norm of $\gamma^{AB}(k)$ remains nonzero everywhere in the Brillouin zone. If the phase of this $\gamma^{AB}(k)$ does not wind by a nonzero integer multiple of 2π, we consider their gauges to belong to the same gauge class.

We are now in a position to introduce our key idea for the prediction of the switching polarization from system A to B. This is that the wavefunction phases evolve along the physical switching path in a minimal way that preserves the gauge class, so that the switching polarization corresponds to the polarization difference of Eq. (1)

and Eq. (8) with Berry phases ϕ^A and ϕ^B computed with the requirement that the two gauges belong to the same gauge class. Crucially, the branch-choice ambiguity in the individual ϕ^A and ϕ^B is no longer present after the difference is taken.

The generalization to the multiband case is straightforward. We define

$$\gamma^{AB}(k) = \det M^{AB}(k) \tag{12}$$

where $M^{AB}(k)$ is the overlap matrix given by

$$M^{AB}_{mn}(k) = \langle u^A_m(k)|u^B_n(k)\rangle \tag{13}$$

for occupied band indices m and n. The gauges are said to belong to the same class if the phase winding of $\gamma^{AB}(k)$ is zero.

One way to insure that gauges A and B belong to the same gauge class is to align one to the other. In the single-band case, the gauge of B is aligned to that of A by taking $\chi(k) = \mathrm{Im}\ln\gamma^{AB}(k)$, and then letting

$$|\tilde{u}^B(k)\rangle = e^{-i\chi(k)}\,|u^B(k)\rangle\,. \tag{14}$$

As a result, the new $\tilde{\gamma}^{AB}(k)$ is real and positive, so that there is clearly no winding. Similarly, the multiband gauge alignment can be accomplished by carrying out the singular value decomposition of M^{AB} in Eq. (12) as $M^{AB} = V^\dagger \Sigma W$, where V and W are unitary and Σ is positive real diagonal. Then the multiband analog of $e^{i\chi}$ is $U = V^\dagger W$, and the gauge of B is aligned to that of A by the transformation

$$|\tilde{u}^B_n\rangle = \sum_m (U^\dagger)_{mn}|u^B_m\rangle\,. \tag{15}$$

The new overlap matrix is then $\tilde{M}^{AB} = V^\dagger\Sigma V$, whose determinant $\tilde{\gamma}^{AB}$ in Eq. (12) is clearly real and positive, thus eliminating the relative winding of gauge B with respect to A.

C. Discrete k space

In any numerical calculation, functions of k must be sampled on a discrete mesh in k. In this case, we can again align the gauge of B to that of A using Eq. (14) or Eq. (15), and compute the polarization difference via Eq. (8). However, in the discrete case there is a new potential source of ambiguity coming from the need to enforce smoothness with respect to k. After discretization Eq. (7) becomes

$$\phi_\lambda = \mathrm{Im}\ln\det\prod_i M^\lambda(k_i, k_{i+1}) \tag{16}$$

where M is the overlap matrix

$$M^\lambda_{mn}(k_i, k_{i+1}) = \langle u^\lambda_m(k_i)|u^\lambda_n(k_{i+1})\rangle\ . \tag{17}$$

This ϕ_λ is gauge invariant, but only up to an integer multiple of 2π. This is reflected by the Imln operation in Eq. (16), which will only result in a phase in the interval $-\pi < \phi_\lambda < \pi$. If one is interested in this phase on its own (i.e., for computing formal polarization) this makes perfect sense, since it is truly a lattice valued quantity. However, our present goal is to compute the difference in phase between two systems with the requirement that both systems are in the same gauge class. For this purpose it is useful to rewrite Eq. (16) in a form where values outside this interval are possible (with the branch being determined by the gauge). To this end we rewrite Eq. (16) as

$$\phi_\lambda = \sum_i \mathcal{A}_i(\lambda) \tag{18}$$

where

$$\mathcal{A}_i(\lambda) = \mathrm{Im}\ln\det M_\lambda(k_i, k_{i+1}) \tag{19}$$

is a discrete analog of the Berry connection A_k. We choose a sufficiently fine k mesh and a sufficiently smooth gauge so that each $\mathcal{A}_i$ is much less than π in magnitude; then ϕ^A can be unambiguously computed (for the chosen gauge). We then choose the gauge in B to be aligned to that of A. Assuming this also results in a smooth gauge in B, we could then confidently compute ΔP from Eqs. (1) and Eq. (8).

D. Gauge invariant formulation

The procedure described in the last section involved constructing a smooth gauge in A, aligning the gauge in B, and then computing each ϕ_λ via Eq. (18). This represents a straightforward, but also inconvenient, means of applying the same gauge class assumption to a realistic calculation. In this section and the next we will develop an equivalent procedure that is more computationally efficient and does not require explicit construction of smooth or aligned gauges.

First, we note that the value obtained above is equivalent to evaluating Φ as

$$\Phi = \sum_i \Delta\mathcal{A}_i \tag{20}$$

where

$$\Delta\mathcal{A}_i = \mathcal{A}_i(\lambda_B) - \mathcal{A}_i(\lambda_A) \tag{21}$$

is the difference between Eq. (19) evaluated at the initial and final configurations (with the previously discussed gauge choices). At present, it is required that k has been sampled densely enough such that each $\Delta\mathcal{A}_i$ is smaller in magnitude than π.

We next note that the quantity $\Delta\mathcal{A}_i$ is equal to the discrete Berry phase computed around the perimeter

of the rectangular plaquette marked by the green arrows in Fig. (1). To see this, we denote the four corners of this plaquette as $\boldsymbol{q}_1 = (k_i, \lambda_A)$, $\boldsymbol{q}_2 = (k_i, \lambda_B)$, $\boldsymbol{q}_3 = (k_{i+1}, \lambda_B)$, and $\boldsymbol{q}_4 = (k_{i+1}, \lambda_A)$, and refer to it henceforth as plaquette p located at $k_i = k_p$. Defining the overlap matrices

$$M_{mn}^{\langle ij \rangle} = \langle u_m(\boldsymbol{q}_i) | u_n(\boldsymbol{q}_j) \rangle \ , \tag{22}$$

the four-point Berry phase about the loop, traced over occupied bands, is

$$\phi^p = \mathrm{Im} \ln \det \left[M^{\langle 12 \rangle} M^{\langle 23 \rangle} M^{\langle 34 \rangle} M^{\langle 41 \rangle} \right] . \tag{23}$$

This four-point Berry phase is equal to the Berry flux through the plaquette, by the same Stoke's theorem argument used to relate Eq. (2) and Eq. (4). This plaquette Berry flux, ϕ_i, can be seen to be equal to ΔA_i computed with the gauges specified above since the alignment of gauges insures that $M^{\langle 12 \rangle}$ and $M^{\langle 34 \rangle}$ have real positive determinants, and thus don't contribute to the phase being extracted by the Imln operation. The advantage of computing ϕ^p as in Eq.(23) is that it is completely insensitive to the gauges used to represent the states at any of the four $\mathbf{q}_i$.[8] Using Eq. (20) we can write Φ as the sum over plaquette Berry fluxes,

$$\Phi = \sum_p \phi^p \, . \tag{24}$$

As the Imln operation suggests, ϕ^p is only gauge invariant up to an integer multiple of 2π, so the above formula still requires that the k-mesh spacing be fine enough that each $|\phi^p| < \pi$ for all k_p, just as was required for ΔA_i.

E. Berry flux diagonalization

With Eqs. (1), (23) and (24), one can compute the polarization difference using arbitrarily chosen gauges for systems A and B. However, there is still a requirement that the k-mesh be fine enough that all ϕ_p in Eq. (24) are smaller in magnitude than π. For a single-band system, this typically does not require a mesh any finer than that needed to compute ϕ_λ from Eq. (16). However, the plaquette Berry fluxes ϕ^p from Eq. (23) are traced over all occupied bands, so their values can quickly grow much larger in magnitude than π when many bands are contributing.

We can instead decompose each plaquette flux into a sum $\phi_p = \sum_n \phi_n^p$ of smaller gauge-invariant phases ϕ_n^p, where n runs over the number of occupied bands. These are the multi-band Berry phases or Wilson loop eigenvalues of plaquet p, obtained from the unitary evolution matrix $\mathfrak{U}_p$ acquired by traversing the boundary of the plaquette. Explicitly,

$$\mathfrak{U}_p = \mathcal{M}^{\langle 12 \rangle} \mathcal{M}^{\langle 23 \rangle} \mathcal{M}^{\langle 34 \rangle} \mathcal{M}^{\langle 41 \rangle} \tag{25}$$

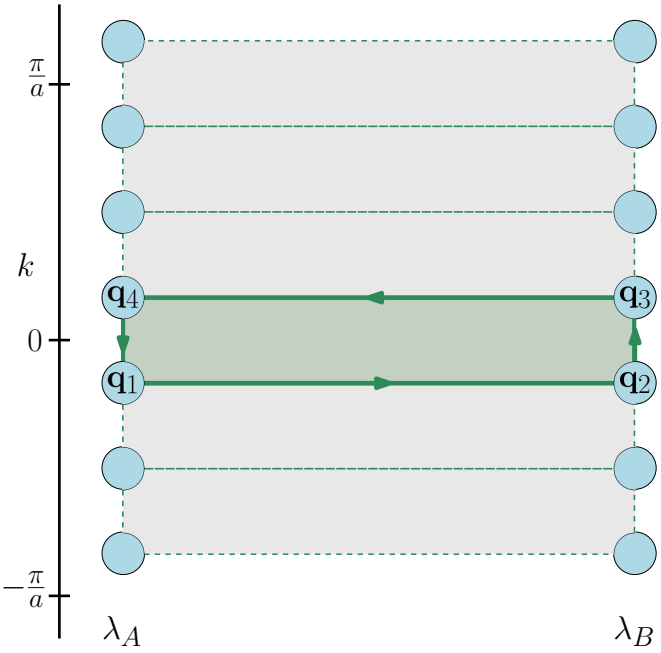

FIG. 1. Sketch of the joint (k, λ) space for computing a change in polarization between λ_A and λ_B. Blue circles represent points where Bloch wavefunctions have been computed. The light grey box represents the surface S that is integrated over in Eq. (2). Dotted green lines represent the plaquets i and the solid green lines represent the path on which the parallel transport procedure is performed around the green plaquet it encloses to obtain its contribution to $P^B - P^A$.

where $\mathcal{M}^{\langle ij \rangle}$ is the unitary approximant of $M^{\langle ij \rangle}$, that is, $\mathcal{M} = V^\dagger W$ where

$$M = V^\dagger \Sigma W \tag{26}$$

is the singular value decomposition of M. The eigenvalues of the unitary matrix $\mathfrak{U}_p$ are of the form $e^{i\phi_n^p}$, providing the needed ϕ_n^p, which are gauge-invariant. Since $\mathrm{Imln} \det \mathfrak{U}_p$ is taken as the Berry flux through plaquet p, we have in a sense diagonalized this Berry flux by obtaining the eigenvalues of $\mathfrak{U}_p$. Finally, the ϕ_n^p can be summed over all plaquettes to obtain the total polarization difference via

$$\Phi = \sum_p \sum_n \phi_n^p \, . \tag{27}$$

This is our central result.

For the method to be applicable the two states λ_A and λ_B must be similar enough that the singular values in Σ do not become too small (this corresponds to the continuum-case requirement that the norm of γ^{AB} in Eq. (11) should remain nonzero). For agreement with the continuum case the individual ϕ_n^p must each be much smaller in magnitude than π. This condition is typically satisfied with a k-mesh density appropriate for a standard Berry-phase polarization calculation, but the density of the k mesh could be increased if necessary. These conditions are further discussed in Section V C.

The above expressions were all written for the one-dimensional case for the sake of simplicity; the generalization to two and three dimensions is quite straightforward. Just as is typically done for the computation of the Berry-phase polarization, the computation is carried out separately for each string of k-points in the direction of the desired polarization component, and the results are then averaged over the complementary directions.

Note that while the computation of overlap matrices between neighboring k-points is quite routine, this procedure also requires overlaps between wavefunctions of corresponding k-points at different λ values (typically different structures). The implementation details for this procedure are discussed in Sec. III.

F. Ionic contribution and alignment

Up to this point, we have focused only on computing the electronic contribution to the change in polarization for already fixed choices of unit cells at each λ. Differences in origin choice and cell orientation between λ_A and λ_B can alter the Bloch function overlaps in Eq. (17).[9] The berry flux diagonalized method is most robust when structures are aligned to maximize overlaps, and thus keep elements of the Σ matrix in Eq. (26) (the singular values) from becoming too small. We make this choice of unit cell by first aligning the structures to minimize the root mean squared displacements of the ionic coordinates. After this initial alignment, we further refine the choice of origin by translating along the polarization direction to maximize the smallest of all the singular values encountered while scanning over all k-points in the above-described procedure. This additional refinement can be performed without additional first-principles calculations using the existing wavefunctions; in the plane-wave representation this is accomplished by computing

$$M_{mn}^{(AB)}(\mathbf{k}) = \langle \psi_{m\mathbf{k}}^{A} | T_\tau \, \psi_{n\mathbf{k}}^{B} \rangle = \sum_{\mathbf{G}} C_{m,\mathbf{G}+\mathbf{k}}^{(A)*} C_{n,\mathbf{G}+\mathbf{k}}^{(B)} e^{-i\mathbf{G}\cdot\tau}$$

where T_τ is the extra translation by τ and the $C_{n,\mathbf{G}+\mathbf{k}}$ are the plane wave coefficients.

The ionic contribution to the polarization change is given by

$$\Delta \mathbf{P}_{\text{ion}} = \frac{e}{V_{\text{cell}}} \sum_i Z_i \Delta \mathbf{r}_i \tag{28}$$

where Δr_i is the displacement of ion i between states λ_A and λ_B.

III. METHODS

The Berry flux diagonalization method is a post-processing step for wavefunctions generated by first-principles density-functional-theory codes. Our current implementation of the method, available at github.com/jrbp/berry-flux-diag, is for wavefunctions in a plane-wave basis. Here we perform calculations in ABINIT using the norm conserving scalar relativistic ONCVPSP v0.3 pseudopotentials with the LDA exchange correlation functional.[10] The necessary overlap matrices are computed from the NetCDF wavefunction files produced by ABINIT, read using the abipy library[11] (https://github.com/abinit/abipy). Th pymatgen library[12] is used in the process of computing the ionic contribution.

We validate and demonstrate the Berry flux diagonalization method as follows. First, we use the method to compute the switching polarization of the prototypical ferroelectric perovskite oxides $BaTiO_3$, $KNbO_3$, and $PbTiO_3$, for which the computation of the switching polarization by existing methods is straightforward. We then use a $2 \times 2 \times 1$ supercell to compute the switching polarization of pure $PbTiO_3$ and of $PbTi_{0.75}Zr_{0.25}O_3$ to demonstrate how difficulties in resolving the branch choice faced by other approaches due to the small polarization quantum do not arise in the Berry flux diagonalization method. The atomic positions in $PbTi_{0.75}Zr_{0.25}O_3$ were taken to be the same as in the pure system.

IV. RESULTS

The computed switching polarizations for the prototypical ferroelectric perovskite oxides $PbTiO_3$, $BaTiO_3$, and $KNbO_3$ are 0.26 C/m^2, 0.29 C/m^2 and 0.77 C/m^2 respectively, in agreement with the established first-principles literature and experimental observations.[13] In this section, we give a detailed analysis of the results for pure $PbTiO_3$, which has the largest polarization and thus presents the most difficult test case. We do this for three cases, namely in the primitive 5-atom cell, in a $2 \times 2 \times 1$ supercell, and in the same supercell but with one Ti replaced by Zr.

The key quantities here are the Wilson loop eigenvalues, which are summed in Eq. (27) to obtain the change in polarization. For $PbTiO_3$, the distribution of the Wilson loop eigenvalues is shown in Fig. 2 for plaquets along the string of k-points corresponding to $k_x = \pi/4a, k_y = \pi/4a$ for the primitive cells, and to the corresponding point $k_x = \pi/2a, k_y = \pi/2a$ for the supercell systems. All Wilson loop eigenvalues are found to be much smaller in magnitude than π, mostly clustered around zero, with a bias in the direction of the electronic polarization change. Here this is negative given the choice of initial and final states.

Each individual contribution to the change in polarization for the supercell is identical to that of the primitive cell, except that they appear with multiplicity four due to the translational symmetries that were lost in the supercell system. So, while the change in dipole moment for the supercell is four times as large as that for the primitive unit cell, and is thus significantly larger than the 2π

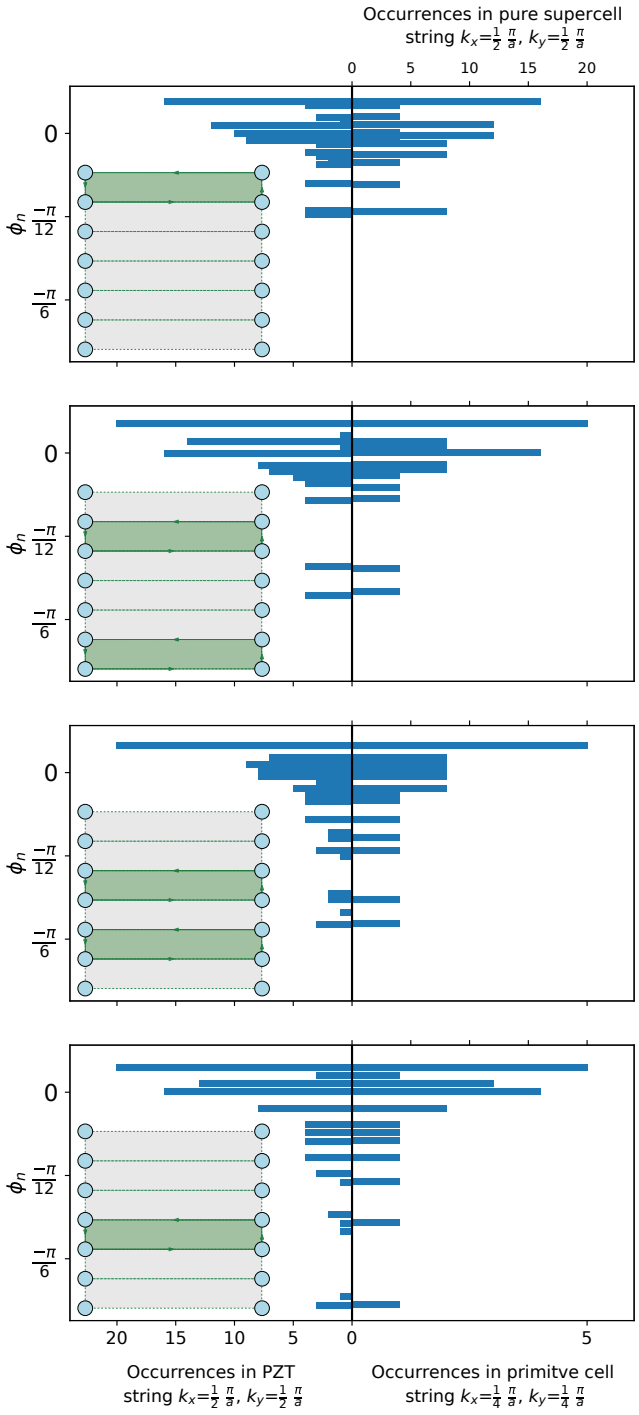

FIG. 2. Histogram of Wilson loop eigenvalues (ϕ_n^p from Eq. (27)) for the plaquets highlighted in the insets following the form of Fig. 1. In each of the two middle plots, the two highlighted plaquets have identical contributions due to time reversal symmetry. Values for pure $PbTiO_3$ are shown on the right. The occurrences of values for the primitive and supercell systems differ only by a factor of 4 as indicated by the two axis scales at the top and bottom of the figure. Values for $PbZr_{0.25}Ti_{0.75}O_3$ are shown at left.

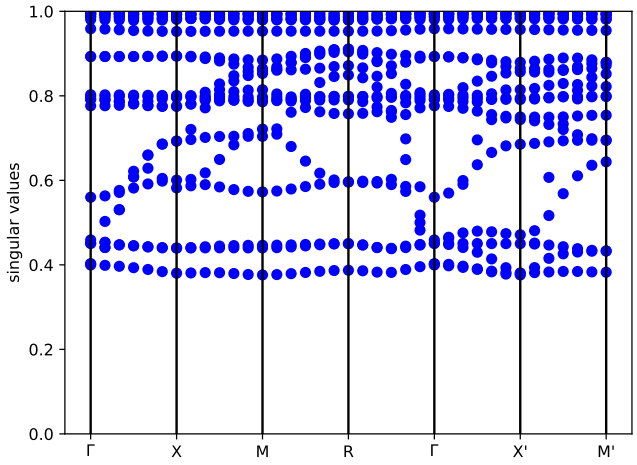

FIG. 3. Singular values throughout the Brillouin zone for $PbTiO_3$, sampled on a 12x12x12 Γ centered k mesh.

phase ambiguity, this does not present any difficulties in the Berry flux method.

The Wilson loop eigenvalues for the system with one Ti replaced by Zr is shown in the left portion of Fig. 2. All eigenvalues fall in the same range as the pure $PbTiO_3$ system, but with some splitting of values. The switching polarization for the system with Zr was found to be 0.762 C/m^2 compared to the slightly larger 0.771 C/m^2 of the pure system.

In Fig. 3, we show the singular values of overlap matrices M between initial and final states at corresponding k-points for $PbTiO_3$ in its primitive cell. These singular values are the diagonal elements of Σ from Eq. (26). If the singular values do not approach zero at any point in the Brillouin zone, the computed information for initial and final states determines the polarization change within the same gauge class assumption. Fig. 3 shows that the singular values for $PbTiO_3$ are well behaved.

V. DISCUSSION

A. Comparison to fictitious path approach

In this section we compare the Berry flux diagonalization method to the commonly used fictitious path approach, using $PbTiO_3$ in its primitive cell and in a 2×2×1 supercell as illustration.

For the fictitious path approach, we choose a simple linearly interpolated path between oppositely polarized states. Fig. 4 shows the formal polarization which is determined modulo the polarization quantum, computed at points along the path for two different sampling densities. Starting with an arbitrary choice for the initial state, the branch is chosen by connecting to the closest value for the next sampled state along the path. The difference between the final and initial states is then divided by

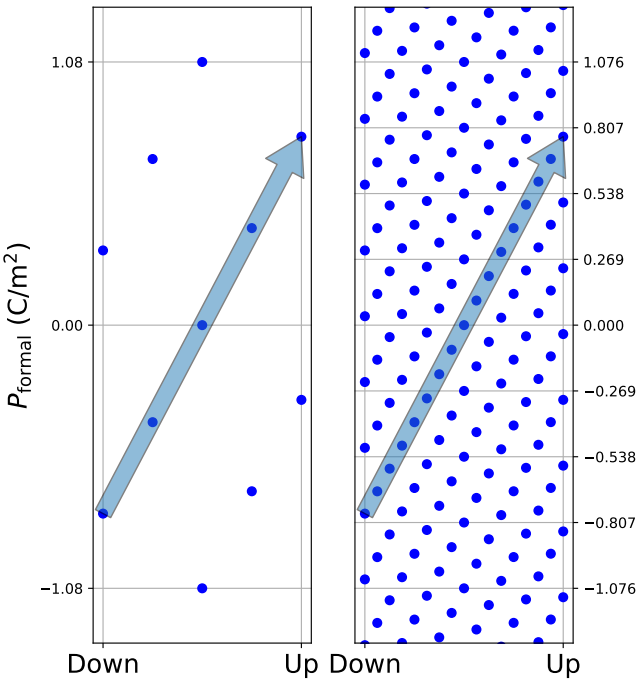

FIG. 4. Evolution of formal polarization of $PbTiO_3$ along a linearly interpolated switching path for the primitive cell (left) and a $2 \times 2 \times 1$ supercell (right). Ticks and horizontal lines mark the polarization quantum. The blue arrow indicates the change in polarization, which with the Berry flux diagonalization method only requires calculations in the initial state and symmetry-related final state.

two to get the spontaneous polarization.

For the case of the primitive cell, calculations for three intermediate states on the path are needed correctly to resolve the branch ambiguity. In the case of the supercell, because of the four-fold decrease in the polarization quantum, the number is significantly larger: 15 intermediate calculations must be done to resolve the branch ambiguity. The Berry flux diagonalization approach in both cases, shown by the blue arrow, predicts the change in polarization (with the correct branch choice) using only the wavefunctions in the initial and final states.

We note that other approaches have been discussed that utilize partial information in addition the evolution of P_{formal}, such as nominal valence charges and Born effective charges. This additional information can help determine the choice of polarization value at the next point on the path even when this is not the smallest change, reducing the sampling density needed. However, the implementation tends to be ad-hoc and is not suitable for automated high-throughput applications. Furthermore, such approaches may not be reliable in situations where these assumed charges are not constant through the switching process.

B. Relation to Wannier functions

The Wilson loop eigenvalues ϕ_n^p used in Eq. (27) and shown in Fig. 2 have a close relation to maximally localized Wannier centers. The parallel transport formalism used to obtain these ϕ_n^p is precisely the same as that used to obtain maximally localized Wannier centers in 1D systems. Such maximally localized Wannier centers are obtained by performing this procedure not across the plaquets discussed in Sec. (II D), but by the loop formed by traversing the Brillouin zone at a given λ. The resulting Wilson loop eigenvalues are then the maximally localized Wannier centers corresponding to a set of Wannier functions (given by their corresponding eigenvectors) which diagonalize the position operator, and sum to compute the formal polarization.

In an analogous way the Wilson loop eigenvalues used in the Berry flux diagonalization method correspond to a set of eigenvectors which diagonalize contributions to a "change in position." The Wilson loop eigenvalues being used here are summed to compute the change in formal polarization.

C. Conditions for applicability

To make any branch choice and compute the change in polarization, some assumption about the dynamics of the switching process must be made. In the method presented in this work, the assumption is that the system evolves in some minimal way between oppositely polarized states. Ionic contributions to the change in polarization are separated by assuming displacements are minimized, and electronic contributions are separated by assuming single-particle wavefunctions evolve into those which have maximal overlap across changes in λ. Such assumptions can fail or become difficult to satisfy for certain systems.

This regime where the technique breaks down can be detected automatically. When the changes in the electronic states across changes in λ becomes large, the overlaps in wavefunctions become small, and some singular values of the Σ matrix of Eq. (26) approach zero. The implementation of the method checks to make sure that no singular values anywhere in the Brillouin zone fall below a threshold (see Fig. 3). Numerical experiments have shown that a threshold of around 0.15 seems to work well for systems tested. There is of course also a branch ambiguity if the Wilson loop eigenvalues (ϕ_n^p of Eq. (27)) have magnitudes close to π. In practice, we have found no cases where this happens without the requirement on the singular values failing first. This can be understood from the viewpoint that the Wilson loop eigenvalues are related to displacements of Wannier centers, with a value of π corresponding to a single charge moving by half a unit cell. When the charge is moved over such a distance the overlaps tend to become small, especially in an insulating system where states are localized.

For such systems, one can revert to constructing intermediate states along λ. If each change in polarization is computed using the Berry flux diagonalization method, λ can be sampled more coarsely than methods that track only the total phase. However, in doing so one should beware of making possibly unsafe assumptions about the dynamics of the switching process.

VI. CONCLUSION

The Berry flux diagonalization method presented here provides a way to compute the change in polarization that is more easily automated, as well less computationally expensive, than existing approaches. The magnitudes of the singular values obtained in the course of the calculation provide a built-in test that the two systems being compared are sufficiently similar that a class of minimal paths producing the same change in polarization can be inferred. Future work will explore the application of this method to the change in polarization between two states that are not symmetry related, such as in pyroelectrics, antiferroelectrics, heterostructures and insulators in finite electric fields. It will also be interesting to test the applicability of the approach to different classes of ferroelectrics, such as organic, inorganic order-disorder, charge-ordered, or improper ferroelectrics. Generalizations of the method to the computation of other quantities requiring Berry curvature integration, such as Chern numbers and characterization of Weyl points, should also reward future investigation.

VII. ACKNOWLEDGMENTS

This work was supported by ONR Grant N00014-16-1-2951, ONR N00014-17-1-2770, and NSF DMR-1334428. We would like to thank Don Hamann and Cyrus Dreyer for useful discussions.

[1] M. E. Lines and A. M. Glass, "Principles and applications of ferroelectrics and related materials," (2001), 10.1093/acprof:oso/9780198507789.001.0001.

[2] Karin M. Rabe, "Antiferroelectricity in oxides: A reexamination," in *Functional Metal Oxides* (John Wiley and Sons, Ltd) Chap. 7, pp. 221–244.

[3] Na Sai, B. Meyer, and David Vanderbilt, "Compositional inversion symmetry breaking in ferroelectric perovskites," Phys. Rev. Lett. **84**, 5636–5639 (2000).

[4] R. D. King-Smith and David Vanderbilt, "Theory of polarization of crystalline solids," Physical Review B **47**, 1651–1654 (1993).

[5] David Vanderbilt, *Berry Phases in Electronic Structure Theory: Electric Polarization, Orbital Magnetization and Topological Insulators* (Cambridge University Press, 2018).

[6] Nicola A. Spaldin, "A beginner's guide to the modern theory of polarization," Journal of Solid State Chemistry **195**, 2–10 (2012).

[7] Raffaele Resta, "Macroscopic polarization in crystalline dielectrics: the geometric phase approach," Rev. Mod. Phys. **66**, 899–915 (1994).

[8] Takahiro Fukui, Yasuhiro Hatsugai, and Hiroshi Suzuki, "Chern numbers in discretized brillouin zone: Efficient method of computing (spin) hall conductances," Journal of the Physical Society of Japan **74**, 1674–1677 (2005), https://doi.org/10.1143/JPSJ.74.1674.

[9] Small rotations in going from A to B present no difficulty, since in practice the calculations are done in internal (i.e., lattice-vector) coordinates. For the same reason, a change in strain state presents no difficulties in principle, but can require some attention to the details of indexing of reciprocal lattice vectors.

[10] D. R. Hamann, "Optimized norm-conserving vanderbilt pseudopotentials," Phys. Rev. B **88**, 085117 (2013).

[11] Xavier Gonze, Bernard Amadon, Gabriel Antonius, Frdric Arnardi, Lucas Baguet, Jean-Michel Beuken, Jordan Bieder, Franois Bottin, Johann Bouchet, Eric Bousquet, Nils Brouwer, Fabien Bruneval, Guillaume Brunin, Tho Cavignac, Jean-Baptiste Charraud, Wei Chen, Michel Ct, Stefaan Cottenier, Jules Denier, Grgory Geneste, Philippe Ghosez, Matteo Giantomassi, Yannick Gillet, Olivier Gingras, Donald R. Hamann, Geoffroy Hautier, Xu He, Nicole Helbig, Natalie Holzwarth, Yongchao Jia, Franois Jollet, William Lafargue-Dit-Hauret, Kurt Lejaeghere, Miguel A.L. Marques, Alexandre Martin, Cyril Martins, Henrique P.C. Miranda, Francesco Naccarato, Kristin Persson, Guido Petretto, Valentin Planes, Yann Pouillon, Sergei Prokhorenko, Fabio Ricci, Gian-Marco Rignanese, Aldo H. Romero, Michael Marcus Schmitt, Marc Torrent, Michiel J. van Setten, Benoit Van Troeye, Matthieu J. Verstraete, Gilles Zrah, and Josef W. Zwanziger, "The abinitproject: Impact, environment and recent developments," Computer Physics Communications , 107042 (2019).

[12] Shyue Ping Ong, William Davidson Richards, Anubhav Jain, Geoffroy Hautier, Michael Kocher, Shreyas Cholia, Dan Gunter, Vincent L. Chevrier, Kristin A. Persson, and Gerbrand Ceder, "Python materials genomics (pymatgen): A robust, open-source python library for materials analysis," Computational Materials Science **68**, 314 – 319 (2013).

[13] Yubo Zhang, Jianwei Sun, John P. Perdew, and Xifan Wu, "Comparative first-principles studies of prototypical ferroelectric materials by lda, gga, and scan meta-gga," Phys. Rev. B **96**, 035143 (2017).